



ELSEVIER

Contents lists available at ScienceDirect

Journal of Archaeological Science: Reports

journal homepage: www.elsevier.com/locate/jasrep

Deep in a Paleolithic archive: Integrated geophysical investigations and laser-scanner reconstruction at Fumane Cave, Italy

Nasser Abu Zeid^{a,d,*}, Samuel Bignardi^{e,a,d}, Paolo Russo^b, Marco Peresani^{c,**}

^a Department of Physics and Earth Sciences, University of Ferrara, Via Saragat 1, Ferrara, Italy

^b Department of Engineering, Via Saragat 1, 44122 Ferrara, Italy

^c Department of Humanities, Anthropogenic and Prehistoric Section, University of Ferrara, Corso Ercole I d'Este 32, Ferrara, Italy

^d CRUST: Interuniversity Center for 3D Seismotectonics with Territorial Applications, Italy

^e Georgia Institute of Technology, School of Electrical and Computer Engineering, Atlanta, GA, USA

ARTICLE INFO

Keywords:

3D Electrical Resistivity Tomography
Microtremor
Spectral analysis of seismic noise HVSR
Inversion
Digital laser scanner models
Paleolithic Fumane Cave

ABSTRACT

In this paper we used an integrated geomatics and geophysical investigation to gain insight about the Upper Pleistocene Cave deposit of *Grotta di Fumane*, located near to Verona city, Italy. Geophysical techniques are seldom considered for investigation of Paleolithic sites, mostly because as is typical in such a context, the physical properties of archaeological remains do not possess a clear contrast, with respect to the background and because of their tiny size, are difficult to detect. As such, the main goals of this combined survey is to reconstruct the volume of the Paleolithic deposit, in terms of visible geometry, sediments distribution and thickness, and map the morphology of the inaccessible karst bedrock that still await to be excavated. These are achieved by using laser scanning and photogrammetry techniques, to create a three-dimensional digital model of the visible portion and using Electrical Resistivity Tomography (ERT) to map the resistivity distribution in the subsurface. Additionally, single station passive seismic measurements were used to provide an indirect confirmation of the sediments thickness by inverting experimental spectral ratio of microtremors. Geophysical results delivered valuable quantitative information about sediments texture spatial distribution highlighting areas of major archaeological interest. Such information guided the 2014–2017 excavations and continuo providing support for long-term planning of future interventions. Finally, the integrated methodology used in this specific context will lead the way for the use of latest technologies to setup a new prospective for enhanced online visualization and virtual reality for the benefits of both cultural and scientific outreach.

1. Introduction

Improvements in data acquisition techniques and processing methods in the past 20 years have made the integrated geophysical applications increasingly common in archaeology (Schmidt and Ernenwein, 2011). The obvious advantage is their capability to define, in a completely indirect and non-destructive way, position, extension, and physical properties of anomalous bodies, provided that they possess sufficient contrast with respect to the surrounding environment, to produce measureable effects (Ellwood et al., 1993; Piro et al., 2000; Clark, 2001; Ortega et al., 2010; Papadopolous et al., 2006, 2010; Orlando, 2013).

Normally, in a Paleolithic cave context the most common materials consist of incoherent sediments of variable grain-size. Differently from other targets of archaeological interest, such as, pottery or masonry ruins, which constitute localized anomalies easily detected by

geophysical methods (e.g. magnetometry and Ground Penetrating Radar), the Paleolithic remains contained in such sediments either do not possess clear contrasts in their physical properties or are too small to be detected. Perhaps this explains why, despite these methods have been successfully employed for the investigation of sediments texture in connection to paleo-soils (Abu Zeid et al., 2016), geophysical methods are rarely employed in this specific context. Many Paleolithic deposits are found inside caves, often used by our ancestors as shelters for long-time. Typically, caves are rather confining environments when geophysical instrumentation must be deployed, especially because the investigation depth is tied to the array length of the sensors. To our knowledge, geophysical investigations in Paleolithic caves were so far limited to retrieving the cave geometry and investigate the presence of voids (Beck and Weinstein-Evron, 1997; Jol et al., 2002; Quarto et al., 2007; Shopov et al., 2008). Moreover, neither survey lines nor subsurface models were accurately geo-referenced.

* Correspondence to: N. A. Zeid, Department of Physics and Earth Sciences, University of Ferrara, Via Saragat 1, Ferrara, Italy.

** Co-corresponding author.

In this view, the Paleolithic site of Fumane represents an opportunity to create a framework for the improvement of geophysical prospecting in such a peculiar context.

The site has been excavated for nearly 30 years and yet, barely half of the deposit has been excavated so far. Therefore, we knew in advance that the sedimentary layers constituting the Paleolithic deposit are characterized by different textures. In the present study, a detailed geometrical mapping of all visible surfaces, including those made accessible from previous excavations was carried out. Initially, laser scanning and photogrammetry were employed to generate a detailed 3D model of the cave. Subsequently, the geophysical survey investigated the sediments that still awaited to be excavated. The main purpose of this effort was to obtain two- and three-dimensional (2D and 3D) models of the distribution of the sediment's geophysical properties and thus their geometry. Of primary interest was the estimation of the residual thickness of the deposit. Among the candidate geophysical techniques suitable for this investigation, we selected the Electrical Resistivity Tomography (ERT) and passive seismic (i.e. microtremor) methods. The ERT technique investigates the electrical resistivity, a well-known physical property for its sensitivity to texture, mineralogical composition and saturation. Further, since modern algorithms can handle a very rough topography, electrodes could be installed even at vertical/sub-vertical surfaces of the deposit. The aim of this prospecting was to obtain a 3D resistivity model of the entire sedimentary stack.

In ERT, the maximum investigation depth is inherently a small fraction of the maximum array length and/or grid size (e.g. Roy and Apparao, 1971), while spatial resolution strongly decreases with depth. To achieve the best compromise between resolution and maximum depth in such a confined space, for the data acquisition we combined the Wenner-Schlumberger and the Pole-Pole electrode arrays. In this way we could leverage on the best resolution in the shallowest 2–2.5 m provided by the first, and the increased investigation depth conveyed by the second. Indeed, bearing in mind that the ratio between depth and poles distance (A-M) is about 0.86 (Oldenburg and Li, 1999), the investigation depth has approximately reached 10 m. Aware of the poor vertical resolution of the Pole-Pole array, and the consequent uncertainty in the correct collocation of the rock-deposit interface, we experimented the use of Horizontal-over-Vertical Spectral Ratio method (HVSr; Nakamura and Ueno, 1986; Nakamura, 1988, 1989, 2000, 2008, 2019) as a tool to confirm the actual thickness of the Paleolithic sediments. The latter method is in fact very sensitive to the elastic impedance variations. The HVSr is based on the spectral analysis of the ambient seismic noise (1–100 Hz) and provides the resonance frequency of the sedimentary stack, which in turn, is intimately linked to the presence of a rocky reflector. The HVSr investigation depth depends on the resonance frequency and the average shear wave velocity of sediments and may even reach down to hundreds of meters. As the name suggests, the ratio between the frequency spectrum of the horizontal to the vertical components of microtremor, is a curve characterized by one (or more) maxima called peaks, whose frequency location is function of the depth of the major elastic impedance discontinuities, while ratio peak value is function of the impedance contrast. In the cave context, the hypothesis is that major impedance discontinuities are connected to either buried rock reflectors (i.e. rocks and stones crumbled from the vault in ancient times), or most likely, to the bedrock/sediments interface. Recent investigations confirmed that the HVSr technique may provide unexpectedly good results concerning the mapping of subtle and shallow sedimentary paleo-soils (Abu Zeid et al., 2016, 2017a, 2017b; Bignardi et al., 2017). Of course, the structure of the cave is expected to introduce lateral effects and 3D reverberations. For this reason, the use of HVSr in such a context is to be considered rather unconventional. Nevertheless, other studies (e.g. Nehmé et al., 2013), although not involving inversion of the HVSr experimental curves, pointed out that the technique can still deliver valuable information on the thickness of the sediments, despite the 3D

nature of the surrounding cave. Additionally, the theoretical response (i.e. amplification) that a cave of similar geometric dimensions would produce can be expected in the frequency range of 1.5 Hz to 3.5 Hz (Lancioni et al., 2014) which, in this cave, should be fairly discernible from the frequency location of the peak related to the sediment/bedrock transition.

Summarizing, the proposed integrated methodology is intended to achieve the following objectives: 1) to execute a high resolution ERT survey to investigate the sedimentary Paleolithic deposit, determine its depth and possibly highlight any structure of interest; 2) to map buried surfaces, so identifying the obstacles to the future excavations and identify voids and/or channels (if any); and 3) to use the HVSr method as an independent tool to confirm the estimated depth of the deposit and indirectly support the Pole-Pole ERT findings.

Concerning the main achievements of this paper: 1) No such a survey has ever been made in the Fumane Cave, which is a very famous and constitutes one of the most important Paleolithic sites in Europe. 2) The geometry reconstructed from the visible surfaces not only represent a powerful tool for dissemination, but also a 3D reference frame in which any finding can be geometrically collocated. 3) We convey a very powerful message: despite the impossibility, in this specific context, of locating anomalies of archaeological interest, geophysical methods can still provide valuable information by highlighting the volumes (i.e. sediment clusters) where tiny remains are most likely to be found, locate hard homogeneous materials (i.e. boulders) that would hinder the excavation, and estimate to which depth a specific portion of the deposit can be excavated before encountering a buried obstacle. These results were indeed provided as a guidance to the archaeological site administrators whose contribution in planning subsequent excavations is highly appreciated.

2. Archaeological and geological setting

2.1. Cave setting

The Fumane Cave is located at 350 m a.s.l. in the Monti Lessini Region (Northern Italy, Verona province) that constitutes a carbonatic plateau tilted to south and dissected by deep gorges (Fig. 1). This archaeological site contains one of the most important Middle and Upper Paleolithic archaeological records in Europe. The cave discovered in 1964 by Giovanni Solinas during the road construction works that intersected the base level of the deposit. The first investigation of the site also dates back to 1964. However, since 1988, the excavation campaigns of the cave are organized regularly every year. The present-day accessible zone of the cave is approximately up to 11 m wide and 22 m long, and when the present geophysical survey was conducted (2013), the top surface of the stratigraphic deposit lied about 3.6 m below the cave ceiling (Fig. 1).

The cave is part of a fossil karst complex formed by erosion during the Neogene. It opens at the base of a carbonatic sandstone cliff (Ooliti di San Vigilio Formation, Upper Lias) composed of alternating massive banks of oolitic calcarenites with typical cross lamination and micritic banks of metric thickness separated from the formers by a discontinuity. In the stream valley where the cave opens, this formation is extensively dolomitized. The karst complex includes a wide cavity, probably a natural pit, filled at the base of the present-day explored deposits with residual dolomitic sands of unknown thickness. Part of the original wall of the pit, located along the eastern sector of the present-day ground level of the archaeological area, is still visible today. The pit walls and the sedimentary deposits preserved on it, were partially eroded as a consequence of the morphological evolution of the stream valley and finally, brought to light thanks to the road construction works. Three tunnels open at the upper levels of the karst complex excavated in the micritic bank. A main (B) and a secondary (C) tunnels form the major rock-shelter, while a third western (A) tunnel connects with B near the cave entrance where the original cave wall is

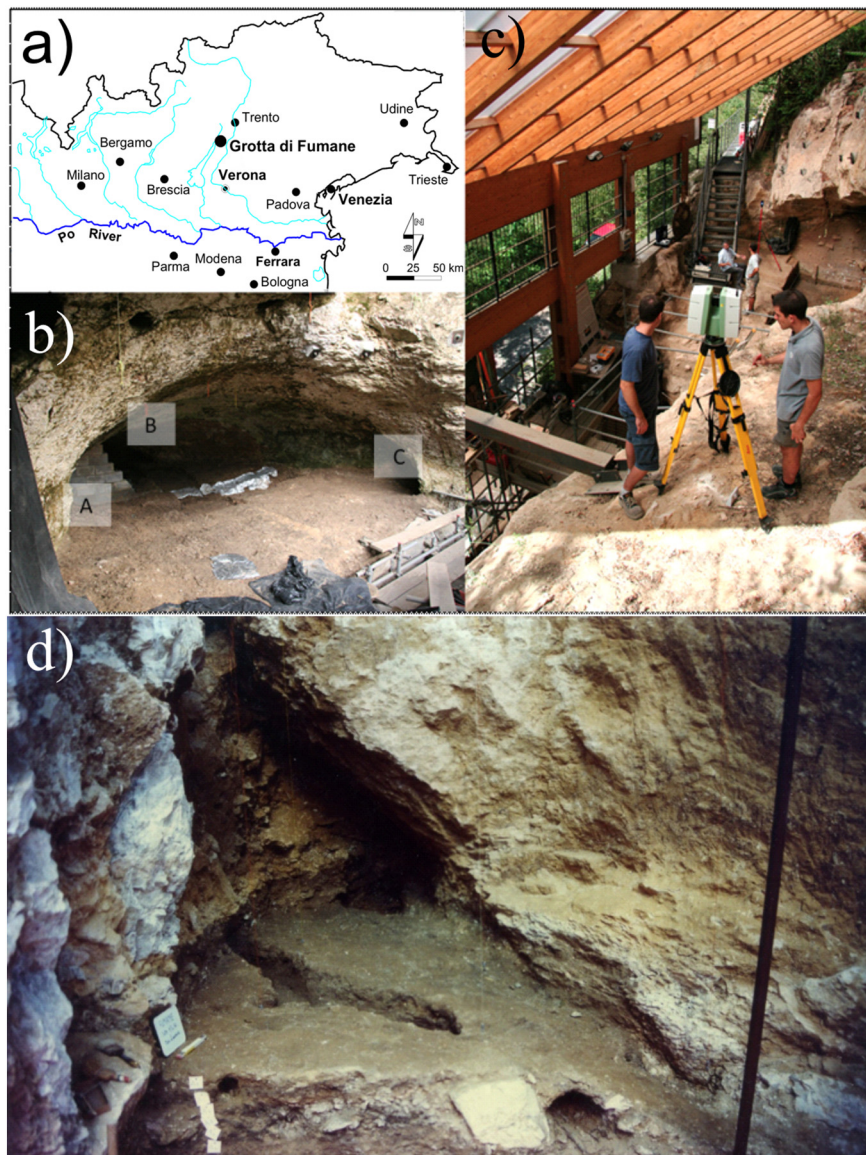


Fig. 1. a) The location of Fumane Cave (North Italy); b) north view of the cave entrance where the ERT survey was carried out and the partially explored tunnels A, B, C are localized; c) instant of laser scanner data collection phase and d) A portion of the entrance of the cave unearthed during excavation in 1989. The section exposes the late Middle Paleolithic sequence from layer A5 down to A10 sealed from the coarse deposits visible on the left.

still visible (Fig. 1). Tunnel A and the left cave-mouth portion of tunnel B form a vault in the calcarenitic bank, still unstable, due to several fractures running roughly parallel to the rock wall that overhangs the cave. The large blocks and slabs which were removed during past excavation campaigns (1988–1996) suggest that the cave entrance was originally positioned few meters south with respect to the present, and that was progressively reduced due to multiple collapses occurred on the main stratigraphic section (still visible at the entrance of tunnel A). Today, a sheltered entrance of almost 30 m² opened at the level of the latest Aurignacian layers lead access to the site. Therefore, the present-day morphology of the cave is the result of the combined action of huge collapses, caused by repeated frost actions, which affected the massive banks and weathering of the micritic bank.

2.2. The sedimentary sequence and its chronological layout

The whole karst complex including the pit and the tunnels preserves 12 m thick sedimentary sequence explored during archaeological excavation, as measured from the present-day ground (at the level of the

road) to the top above the cave entrance. Four macro-units: S, BR, A and D) have been distinguished based on lithology and archaeological remains contents (Bartolomei et al., 1992; Fig. 2). Sedimentary features are currently accessible from: the main cut facing the road (residual-base sands, macro-units S and BR); the three sections of the pit opened in 1992, 1993 and 1995 (lower boulders above the residual sand and units from S10 to A3); the section at the entrance of tunnel A (from A9 to D1e); the sections in cave-mouth (from A9 to D1e and A6 to D1e); the walls of the trench opened in 1989 and 1990 in the entrance of the cave (layers A12 to A10); the small section preserved at the entrance of tunnel C (layers A9 to D6). Based on the geometry of visible sections of such geological bodies the sedimentary component was estimated to be approximately 220 m³ (where: length ~ 11 m, width ~ 5 m and thickness ~ 4 m).

The Paleolithic sequence records the main climatic events occurred in the last glacial cycle which includes a cultural record ascribed, according to the preserved archaeological contexts in distinct levels, to the Mousterian, Uluzzian, Aurignacian and Gravettian periods. Preliminary assessment based on sedimentological, pedological and

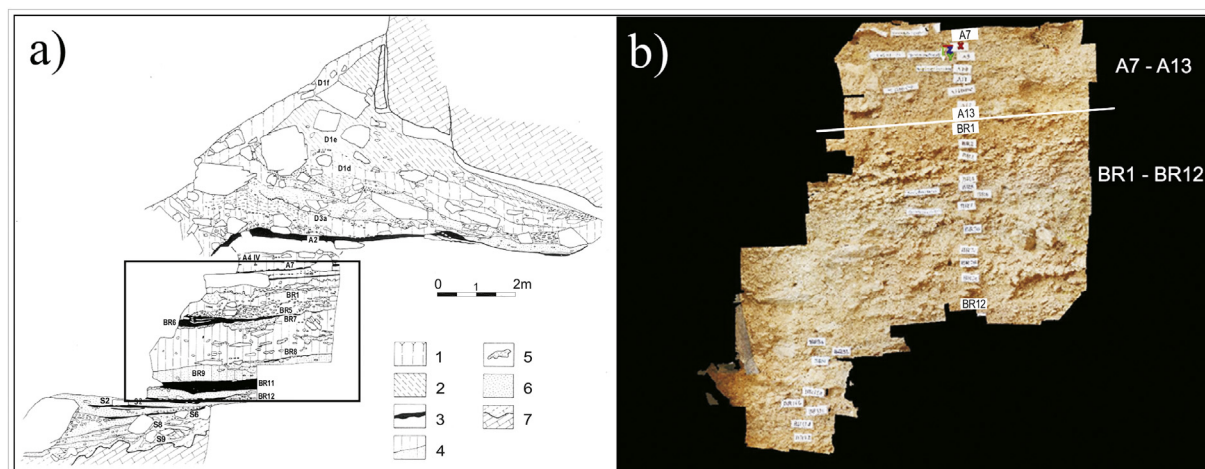


Fig. 2. a) Stratigraphic sequence of Fumane Cave reported for the main sagittal section now partly dismantled with the main lithological features in D, A, BR and S macro-units: 1 — rendzina, upper soil; 2 — slope deposits with boulders; 3 — living floors with high concentration of organic matter or charcoal; 4 — loess and sandy loess; 5 — carbonate cemented layers; 6 — sandy deposits; 7 — unweathered and weathered bedrock (after Peresani et al., 2008); b) photogrammetry reproduction of the main stratigraphic sequence indicated by the rectangle in (a) showing the layers A7–A13 and BR1–BR12.

palaeontological analyses have been reported elsewhere (Cassoli and Tagliacozzo, 1994; Cremaschi et al., 2005; Romandini et al., 2014; López-García et al., 2015).

Above the residual yellow massive dolomite sandy plug, the macro-unit S groups layers made of dolomite sand, angular stones, surface weathered boulders, and traces of human occupation scattered in layers from S10 to S1 for a total thickness of 1.4 m. This differentiation is based on the grade of anthropization rather than on the lithological content. Macroscopic features, grain size, heavy minerals, micro-morphology, and magnetic properties indicate that pedogenesis affected the bedrock in conditions of climatic instability, followed by moderate roof degradation and the hydrological redistribution of the dolomite sands at the end of MIS5 (Martini et al., 2001). The overlying macro-unit BR is a massive sedimentary body made of stones and aeolian dust. Layer BR11 is a 0.4 m thick dense accumulation of cultural material, ungulate bones still articulated, knapped stones, charcoal and associated combustion features. A massive sedimentary body groups units from BR10 up to BR7a for a total thickness of 1.6 m. Units from BR6 to BR4 are coarse open-work frost breccia sealing scattered Mousterian fire-places and associated cultural material (Cremaschi et al., 2005). An increased content in fine fraction features the layers from BR3 to BR1 at the top of macro-unit BR which marks a clear discontinuity with the overlain macro-unit A, due to the looseness and the different sedimentary structure of this latter one. Macro-unit A includes several horizontal layers from A13 to A1 mostly composed of residual dolomite sands (layers A13–A12), angular fine-medium sized stone layers (levels in A10 complex, layers A7, A4), stones, slabs and fine material (layer A3) and variable content of organic and cultural material (A11, levels in A10 and A9 complexes, A6, A2–A1) locally affected by cryoturbation and other deformations (Peresani et al., 2008). The content in sands and aeolian silt increases till becoming almost exclusive from the sheltered area to the exterior. Sediments are generally loose or densely packed, but never intensively cemented. The cave entrance and the main tunnels were sealed from macro-unit D at the top of the sequence. It is mostly composed of boulders resulted from rock falls and of stones, sand and variable content of aeolian dust. Layers thickness gradually reduces moving towards the cave-mouth where post-depositional deformations acted under the influence of periglacial conditions at the onset and during MIS2.

Traces of repeated human frequentations are recorded across macro-unit S, while in macro-unit BR, if we except the dense cultural remains in BR11, this evidence mostly takes the form of dispersed lithic artefacts and faunal remains or hearths with scattered tools and bones

ascribed to short-term occupations (Cremaschi et al., 2005; Peresani et al., 2011). Traces of much more intense human occupation have been inferred from the macro-unit A record. There are Mousterian living floors in A11, A10, A9, A6–A5 (Peresani, 2012; Fiore et al., 2016), Uluzzians in A4 and A3 (Peresani et al., 2016) and Protoaurignacian in A2–A1 (Broglia et al., 2006; Broglia et al., 2009). Evidence of human presence can still be seen in the lowermost layers of macro-unit D, layers D3d, D3b–D3a and D1c, these being the latest Aurignacian units, but it becomes sporadic in the middle level, D1d, where dispersed Gravettian artefacts were recovered.

The part of the sequence still visible today and therefore the object of the geophysical investigations, includes portions of macro unit A (layers A7–A12) and macro-unit BR (Fig. 2). U/Th, TL and a large set of ^{14}C dates prove that the late Mousterian, the Uluzzian, the Aurignacian and the Gravettian fall in the MIS3 and the onset of MIS2 (Peresani et al., 2008; Higham et al., 2009; Martini et al., 2001; Douka et al., 2014).

3. Materials and methods

The first part of this work aimed at constructing a detailed geometrical model of the cave as this model represents a key aspect for the success of the entire geophysical survey. For this purpose a total of 11 scanning positions were selected for data acquisition using a C10 laser scanner (Leica, Switzerland), then merged into a single three-dimensional unique model perfectly georeferenced. This highly detailed geometrical model of the internal structure of the cave, was integrated with a photogrammetric survey using a Canon Eos7D camera of which images were processed with a modern “structure from motion” software, PhotoScan (Agisoft LLC, Russia). While the former was used to generate a dense cloud of points mapping the entire cave surface the latter focused only on areas of major interest and for assigning natural colors to the points from the laser scanner model (Fig. 3c). For further details see (Bolognesi et al., 2014, 2015).

Concerning geophysics, the ERT technique is capable of reconstructing the vertical and horizontal electrical stratigraphy (i.e. resistivity). As this method is often encountered in an archaeological context, a detailed description of the basic principles is beyond of the scope of the present paper. Briefly, a continuous or slowly variable current “ I ” is generated and injected into the ground by means of a pair of metallic electrodes (AB, small nails were used in our case). As consequence, an electrical potential drop is created, whose value “ ΔV ”, is measured at a different electrode pair (MN). In practical realizations, a

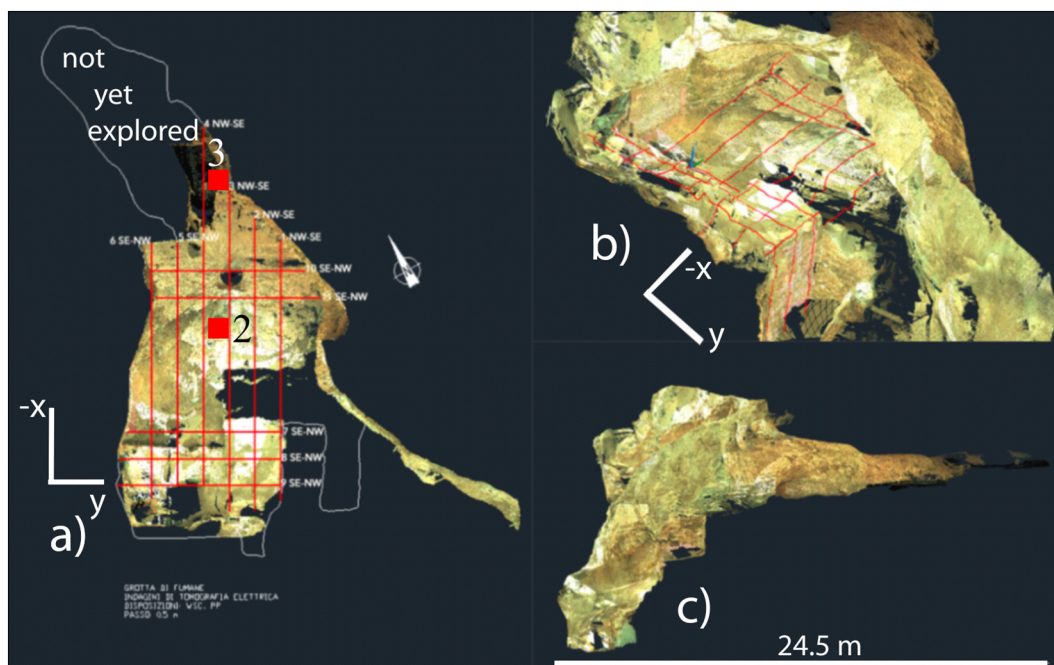


Fig. 3. a) Plain view of ERT profiles (red lines); b) 3D view of the ERT profiles and the reconstructed topographic model of the Fumane Cave; c) picture of the final georeferenced topographic model reconstructed after merging data of 11 different scanning positions. Red squares: position of two of the HVSR tests (numbers 2 and 3) performed at the top of the deposit. Test number 1 (not shown in figure), was conducted at the base of the deposit, near to the cave entrance, on the outcropping bedrock.

set (array) of electrodes is deployed and the measure is performed on all the quadrupole addresses (ABMN) preloaded in a file called protocol or sequence that is automatically executed by the georesistivity meter. The potential drop at each measure pair of electrodes depends on the injected current intensity, distribution of the resistivity in the subsurface, besides the reciprocal positions of all four electrodes. An apparent resistivity ρ_a , calculated as: $\rho_a = k \cdot \Delta V / I$ (Ωm), is obtained for all possible quadrupoles; where, k is the geometric factor and depends only on the reciprocal position of the electrodes forming up each quadrupole. Obtained experimental apparent resistivity data are plotted as pseudosections that are normally used to qualitatively judge the quality of the data. Moreover, the standard deviation of the measured potential difference of our data was always $< 2\%$ (i.e. high quality data). Generally, data are measured along profiles (2D) or on a regular grid (3D). All calculated ρ_a values are used to obtain the spatial distribution of the true resistivity in the subsurface (the resistivity model) through an inversion process. Inversion is a computational method in which the difference between experimental data (ρ_a in this case), and simulated values, is minimized. The scalar valued functional representing such difference is often termed “Misfit”. Minimization of the above-mentioned differences generally leads to an “ill-posed” inversion problem. Often, to insure numerical stability a regularizing term is added to the misfit, leading to the so-called “Energy functional” or “Energy” (Tikhonov and Arsenin, 1977). An iterative regression algorithm is used to modify the resistivity value of each model parameter, through successive approximation, starting from an initial guess to a resistivity distribution (average value) for which the Energy is minimal (Tsokas et al., 2009; Bonsall and Sparrow, 2013). Each iteration involves a finite-element procedure that computes the predicted apparent resistivity values based on the new model parameters.

The geoelectrical survey covered the main excavated area and comprised 6 parallel ERT profiles (ERT1–6, oriented NW-SE) roughly one-meter apart from each other and 7 more (ERT7–11), running in orthogonal direction. Electrodes (small metallic nails) were positioned at fixed distance of 0.5 m. All data were collected using a multichannel geo-resistivity-meter ABEM SAS Inc. 4000 (Sweden). Due to the

irregular shape of the cave, profiles lengths ranged from 6.5 to 12 m (Fig. 3a). In order to maximize the amount of information contained in our data, we leveraged on two different electrode array configurations: Pole-Pole and Wenner-Schlumberger arrays. In this way, we combined the benefits of the augmented investigation depth offered by the former, while retaining the high resolution of the latter.

The apparent resistivity data were inverted using the software ERTLab (2012, www.geoastier.com, www.mpt3d.com). ERTLab features an algorithm based on Occam's inversion strategy to deal with the ill-posedness issue. Further, data outliers are handled using a robust formulation of the misfit functional (Morelli and LaBrecque, 1996). The software comfortably handles rough topography and free surface effects such as those represented by the cave walls. Accounting for these boundary conditions was simple thanks to the availability of a high resolution topographic model. Inversion, preliminarily performed along single 2D profiles (Obradović et al., 2015), was successively extended to the entire dataset and processed with the full 3D approach. Two 3D models were obtained, one for each electrode configuration used.

The HVSR technique is founded on a layered subsurface assumption, where a low velocity sedimentary layer (or stack) rests on a high velocity bedrock. The method is useful to infer the presence of lithological discontinuities characterized by a variation of elastic impedance (i.e. mostly related to changes in shear waves velocity while density contribution is actually minimal). Their properties are manifested as one or more peaks in the resulted spectral ratio curve. In particular, the most significant peak is usually associated with the sediments-bedrock transition and a simple relation exist between the depth of the interface, the frequency location of the peak, and the average shear wave velocity of the sediments. The method is straightforward, easily applied and widely known in microzonation studies (Bard, 1998; SESAME, 2004; Mantovani et al., 2019). Microtremor data can be collected by compact and user-friendly equipment featuring a seismograph connected to a short-period three-component seismometer.

Obviously, the complex geometry of the cave, which violates the 1-D assumption may impact the meaningfulness of the HVSR curve (Bignardi et al., 2013, 2014). Nevertheless, it could be argued as well

that if a peak is indeed encountered in the experimental HVSR curve, this is most probably connected with either the proper vibration frequency of the cave structure or with a lithological discontinuity located at some depth below the ground surface. Despite the fact that both seem to be reasonable explanations, a theoretical evaluation of the proper frequency of the Fumane Cave shows that the expected frequency range of such a structure ranges between 1.5 Hz and 3.5 Hz (i.e. less than the resonance frequency of the Paleolithic deposit). Moreover, while preliminary microtremors-based studies in very complex subsurface models seem to point out that reflector steepness do introduce a small frequency shift on the horizontal components of motion (Matsushima et al., 2014a, b; Dietiker et al., 2018; Dietiker and Hunter, 2019; Bignardi et al., 2019), the frequency of the peak can still be retained reliable enough for our purpose of inferring a good estimate of the bedrock depth. Indeed, provided an average value of the Vs velocity of the sedimentary stack is available, since the bedrock is sufficiently shallow we consider the uncertainties acceptable (Bignardi, 2017). Further, HVSR curves were inverted using the code “OpenHVSR” (Bignardi et al., 2016, 2018a, 2018b) which retrieves one-dimensional model parameters (i.e. Vs and thickness) that best fit the resonance frequency peak.

The passive seismic data (i.e. microtremor) were collected using a three component 2 Hz electromagnetic seismometer connected to a 24-bit seismograph model Vibralog (M.A.E., Italy). One hour long recordings, sampled at 250 Hz, were collected at three selected points (red squares in Fig. 3a), one was placed over the outcropping bedrock near the cave entrance.

Microtremor signals were processed using the software Geopsy (www.Geopsy.org) (Di Giulio et al., 2006) and a set of HVSR curves was obtained. For the processing we followed the standard procedure, reader can refer to the SESAME (2004) guidelines. Concerning the processing parameters, microtremor recording were split in windows of 30 s, 50% overlap and 5% cosine tapered. The combined horizontal spectrum was computed using the RMS. Finally, we used the Konno and Ohmachi (1998) smoothing window with $b = 40$.

4. Results

In Fig. 4a we present as an example the Pole-Pole 2D resistivity inversion model of profile No. 4, while in Fig. 4b the 800 Ω·m iso-resistivity surface is illustrated. We infer that this surface identifies the morphology of the high resistivity bedrock. It gently dips towards north, however, it is recognized to possess a complex morphology once the 3D elaboration is considered (Fig. 4b). In addition, it shows that the

depth to the bedrock ranges between 5 and 6 m below the 2013 walking surface. Moreover, the 2D section (Fig. 4a) shows low resistivity values ($< 100 \Omega\cdot m$) in the first three meters which represents the zones of greatest interest because they may contain fine-grained supported materials. Such locations will be considered of high priority for future excavations.

Detailed mapping of these low resistivity volumes was obtained from the 3D inversion resistivity model from Wenner-Schlumberger apparent resistivity data (Fig. 5a). The Figure shows the volumes with resistivity lower than $75 \Omega\cdot m$. The elongated geometry follows the principal longitudinal axis of the cave. In Fig. 5b–d, three selected depth slices are shown. They reflect the spatial resistivity variation in the top 2.5 m of the deposit. The shallowest shows four anomalies with high resistivity values which we interpreted as local troughs filled with drained coarse-grained sediments. The features of main interest, however, are the portions with resistivity lower than $75 \Omega\cdot m$ which extend to the maximum investigation depth, about 2.5 m below the 2013 walking surface. We interpreted these areas to be rich with clasts supported by fine-grained materials where it is likely to find archaeological remains. In Fig. 5c, the resistivity slice shows the presence of values similar to those shown in Fig. 5a which suggests the presence sediments with fine-grained texture elongated towards tunnel C (Fig. 5c), furthermore, this resistivity slice indirectly hypothesis that the depth to the rock is not yet reached as low resistivity values still predominate.

Concerning the results from microtremor, in Fig. 6a we show the experimental HVSR curves of the three tests performed. Despite the fact that multiple peaks are present, two of them at about 15 Hz and 38–40 Hz are compatible with the results from the ERT and correspond to an estimated depth within the sedimentary stack. Quantitative interpretation accomplished through inversion of the HVSR curves provided results both in the data space (i.e. the curve fitting: Fig. 6a–c) and in the parameter space (the vertical Vs profiles: Fig. 6d–f). Of course, since available modelling routines assume the subsurface to be represented by stack of infinite parallel layers (i.e. 1D assumption), which is an acceptable approximation only when lateral variations are much greater than the wavelengths into play, to achieve a good fitting with experimental HVSR curves was particularly challenging. As mentioned above, 3D effects are expected to be not negligible in complex geometry such as this case (Guéguen et al., 2007; Compare et al., 2009; Bignardi et al., 2013, 2014), therefore, inversion was not able to retrieve the exact shape and peak amplitude of the experimental HVSR curves. Fortunately, in the HVSR context, the amplitude of the peak is of secondary importance, the most relevant parameter being its frequency position, which, all considered, was actually fitted in an acceptable

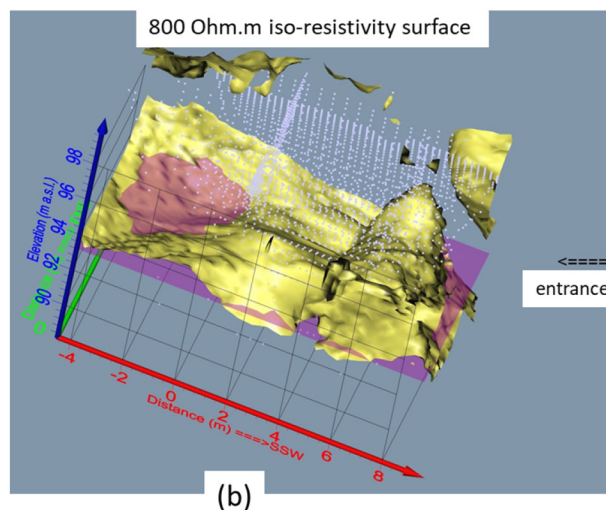
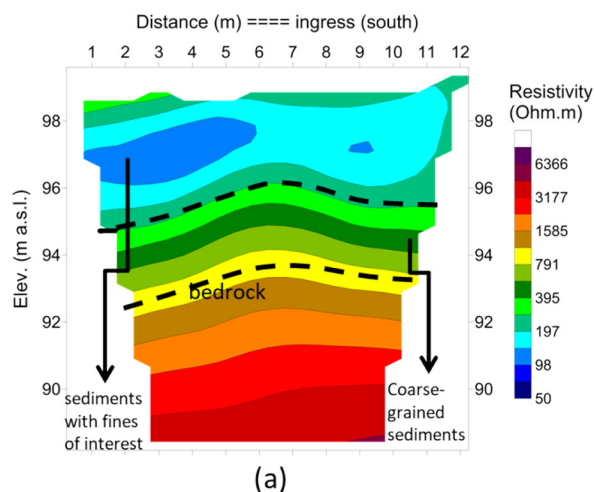


Fig. 4. a) Pole-Pole 2D inversion resistivity model (profile ERT4) and b) Pole-Pole 3D resistivity model showing the 800 Ω·m iso-resistivity surface. The purple slice shows the 93.5 m a.s.l. depth surface that intersects the iso-resistivity surface confirming that that bedrock depth in this area is > 5 m.

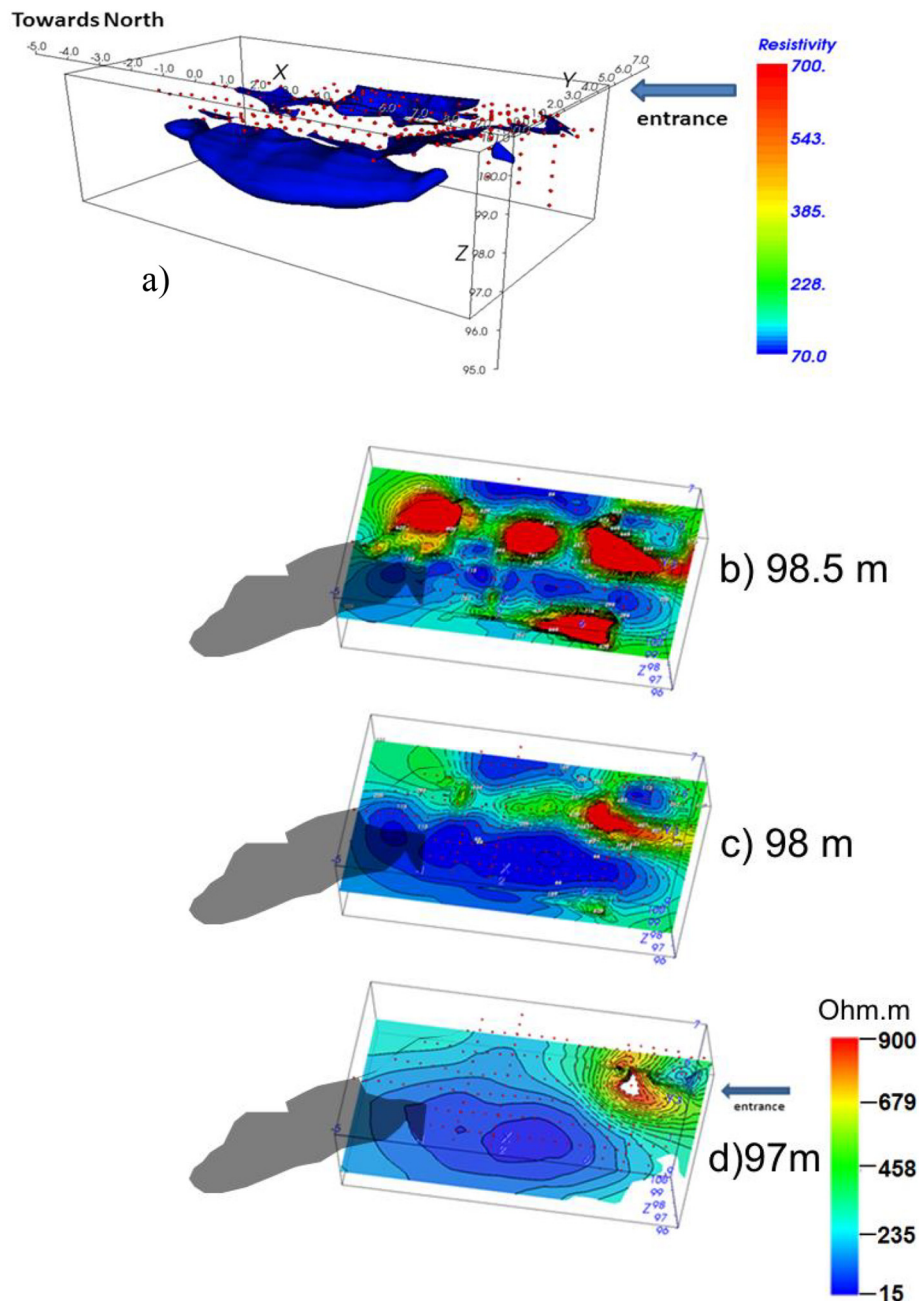


Fig. 5. 3D resistivity images of the investigated stratigraphic deposit as viewed from west. The depth axis represents absolute elevation (m a.s.l.). a) Three dimensional representation of low resistivity volumes ($< 75 \Omega\cdot\text{m}$) considered to be of high archaeological interest. Resistivity depth slices at: b) 98.5 m a.s.l.; c) 98.0 m a.s.l. and d) 97.0 m a.s.l. Red dots: spatial locations of true resistivity values. Shaded area: inaccessible portion of the Fumane Cave not yet explored.

way. The retrieved velocity profile near the cave entrance (i.e. at the base of the excavated portion of sediments) is compared to those obtained from data collected at the top of the Paleolithic deposit (Fig. 6b–c). Bearing in mind that the models refer to the local geology below the seismometer, it can be inferred that the sediments become thinner towards the inner part of the cave. Further, the Vs models show the presence of a common sharp increase in the shear velocity about 1 m deep. Considering that the two sites have the same elevation, we interpreted this increase in shear velocity as related to a marked lithological boundary separating the macro-units BR and A, where BR1 layer marks the top of the former and layer A12 the base of the latter. Indeed, the layer is actually visible on the exposed section of the deposit towards east (Fig. 2). This result deserves attention as it provided clues about the extension of this lithologic discontinuity also beneath the

central part of the deposit. Having the possibility to sample the surface at consistent numbers of microtremor points will allow mapping both its presence and morphology.

As a final note, the passive seismic results did not provide evidence on the presence of voids or channels across or at the base of the deposit.

After the conclusion of the geophysical survey, the deposit was further excavated. During 2014 and 2017 two field campaigns investigated the nature of the materials that produced the observed resistivity anomalies. In these campaigns 9 m^3 (comprising squares in Fig. 7 numbered as: 80–81, 90–93, 100–103 and 110–112) were excavated. Two stratigraphic complexes A10 and A11 of 0.5 m thick were identified (Peresani et al., 2017). A11 is a dark brown anthropogenic layer that lies on stony compact sediments with sandy-loamy fine fraction (unit A12). A10 is a 40 cm thick sediment consisting of an

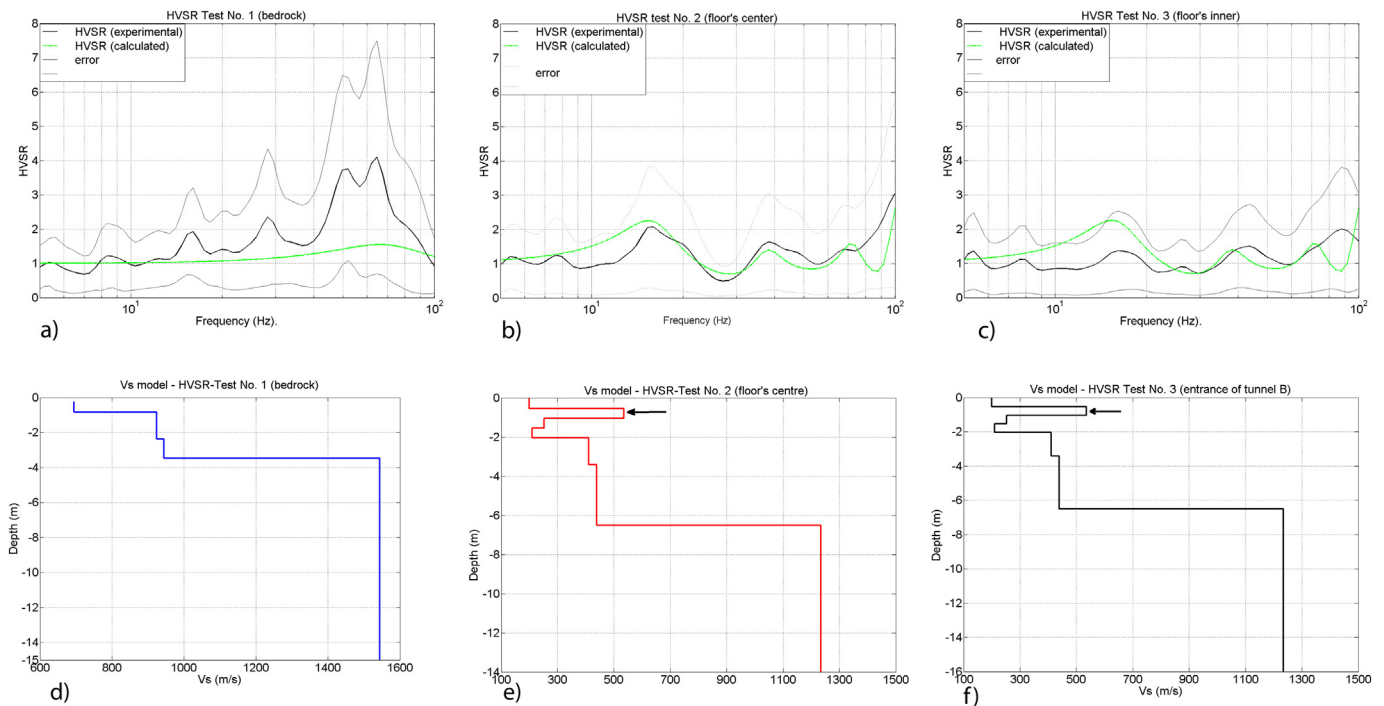


Fig. 6. Results of the HVSR survey: a–c) experimental (black) and theoretical (green) HVSR curves obtained after inversion; d–f) derived 1D shear wave velocity models. Black arrow (e–f): inferred high Vs layer at roughly 1 m depth below the floor area.

alternate sequence of thin (3–4 cm) dark brown levels containing small-medium sized angular stones and amounts of anthropogenic remains (A10I, A10III; A10IV), comparable to A11, with thin levels almost exclusively composed of loose angular medium-large sized stones (A10IBRI, A10IBRII, A10IIIBRIII, A10VBRIV; photo insert in Fig. 7).

5. Conclusions

Prehistoric sites receive little attention by the wider geophysical community, mostly because such contexts lack the features that typically make a geophysical survey straightforwardly successful. In fact, Paleolithic human-made structures and their related remains are small-

sized and sparse to result undetectable in the heterogeneous sedimentary matrix. In the Fumane Cave, long-term excavations have provided materials (such as simple hearts, stone knapping and organic remains) that implicate periodic occupation by humans. The presence of numerous, closely packed archaeological layers and countless remains of tiny size, make any invasive testing (test pits, coring) unpractical. This opens new venues for the implementation of integrated geophysical and topographical surveys.

Our geophysical investigation proved to be successful in mapping the bedrock subsurface morphology as well as providing insight on the nature, thickness and volume of the infilling sediments in a completely non-destructive way, thus delineating appropriate areas of potential

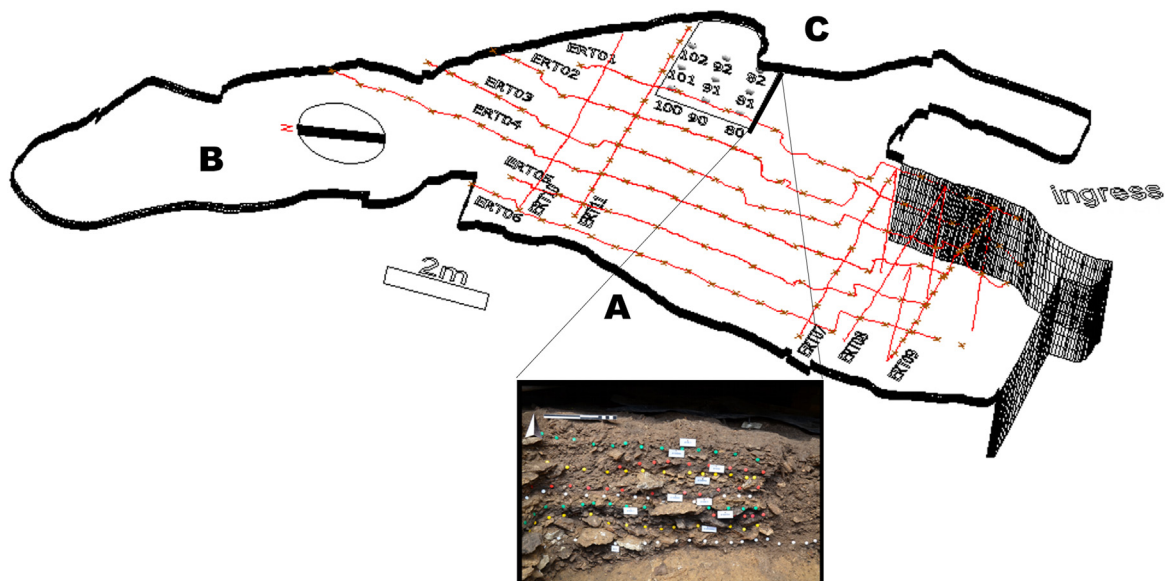


Fig. 7. The stratigraphy of the A10 and A11 contexts exposed during the 2014 and 2017 Fieldwork (picture). The position of this square was suggested to infer the nature of the encountered high resistivity anomaly. A, B and C: other partially explored tunnels.

archaeological interest. On the one-hand, short-term advantages provided by our findings concerned the identification of areas with largest sediments content, i.e. where remains are more likely to be found. The estimated volume of these sediments in the top three meters amounts 50–75 m³. In this way, further excavations could be planned more efficiently. On the other hand, long-term advantages resulted, and the trend is expected to continue, in more goal-focused use of research funds and to aid in the valorization of the effectiveness of the combined use of both geophysical methods (3D ERT and microtremors) and geomatic digital models among the scientific and professional archaeological communities. In this respect, the fact that the excavation campaigns performed during 2014 and 2017 (i.e. after the conclusion of the geophysical prospection) confirmed results produced in 2013 is a very good example.

Recalling that archaeological excavations are inherently destructive, in order to keep track of the remains spatial distribution, it is extremely important to carefully annotate their nature and position. Since the excavation lasts for a long time, a large amount of notes and observations accumulate before the end of each campaign. Georeferencing collected information allows error minimization and most importantly their immediate consultation, integration and correction. This last aspect is of utmost importance as it makes deductions about the interdependence of the remains more feasible in a very short period of time. In this sense, the digital cave model provides a detailed three-dimensional framework to correctly position referenced images of such important features. Further, such a tool naturally integrates the geophysical results so highlights relevant karst structures and sedimentary discontinuities that otherwise would pass unnoticed and would not be accounted in the archaeological deductive process. Additionally, the geometrical shape of exposed surfaces integrated with geo-referenced geophysical results (all performed before excavation) shall be enhanced with the post-excavation geo-referenced information gained on the lithological nature of the sedimentary matrix and distribution of relevant remains. Analysis of such integrated information provides an extremely useful, digital, tool for planning future excavations and drawing scientific conclusions on the deposit evolution across millennia. The ambition of digitally integrating information from different techniques provides also a powerful outreach tool of impressive visual impact to disseminate knowledge and communicate results to a wider professional and non-professional public. The latter is an important point, because, it raises awareness about the importance of prehistoric sites and their role in explaining history and evolution of humans. Finally, this may lead to the development of virtual reality applications that could be shared both with specialists and the wider audience. We think that this work constitutes a further step towards a more interactive information technology, such as virtual reality applications that integrate geophysical aspects and archaeological findings. We like to call this perspective Cyber Paleolithic Archaeology. We are aware that we did not fully realize this milestone but work is going on and we hope that more results will be published in the near future.

Acknowledgments

Research at Fumane is coordinated by the Ferrara University in the framework of a project supported by the Ministry of Cultural Heritage ad Activities — Veneto Archaeological Superintendence, public institutions (Lessinia Mountain Community — Regional Natural Park, Fumane Municipality), and private associations and companies. Authors' contributions: M.P. designed research; N.A.Z., geophysical survey planning, N.A.Z., S.B., M.P., geophysical data acquisition; N.A.Z. and S.B., data inversion; M.B., and P.R. performed scanning and photogrammetry. N.A.Z., M.P., S.B., P.R. and wrote the paper. Finally we thank Prof. G. Santarato, Department of Physics and Earth Sciences, for his encouragement during work progress.

References

- Abu Zeid, N., Corradini, E., Bignardi, S., Santarato, G., 2016. Unusual geophysical techniques in archaeology - HVSR and induced polarization, a case history. In: 22nd European Meeting of Environmental and Engineering Geophysics, NSAG-2016, <https://doi.org/10.3997/2214-4609.201602027>.
- Abu Zeid, N., Corradini, E., Bignardi, S., Nizzo, V., Santarato, G., 2017a. The passive seismic technique "HVSR" as a reconnaissance tool for mapping paleo-soils: the case of the Pilastris archaeological site, Northern Italy. *Archaeol. Prospect.* 24 (3), 245–258. <https://doi.org/10.1002/arp.1568>.
- Abu Zeid, N., Bignardi, S., Santarato, G., Peresani, M., 2017b. Exploring the paleolithic cave of Fumane (Italy): geophysical methods as planning tool for archaeology. *SEG Technical Program Expanded Abstracts 2017*, 5125–5129. <https://doi.org/10.1190/segam2017-17729320.1>.
- Bard, P.-Y., 1998. Microtremor measurement: a tool for site effect estimations? In: *Proc. of the 2nd International Symposium on the Effects of the Surface Geology on Seismic Motion*, ESG98, Yokohama, Japan, pp. 1251–1279.
- Bartolomei, G., Broglio, A., Cassoli, P., Castelletti, L., Cremaschi, M., Giacobini, G., Malerba, G., Maspero, A., Peresani, M., Sartorelli, A., Tagliacozzo, A., 1992. La Grotte-Abri de Fumane. Un site Aurignacien au Sud des Alps. *Preistoria Alpina* 28, 131–179.
- Beck, A., Weinstein-Evron, M., 1997. A geophysical survey in the el-Wad cave, Mount Carmel, Israel. *Archaeol. Prospect.* 4, 85–91. [https://doi.org/10.1002/\(SICI\)1099-0763\(199706\)4:23.3.CO;2-3](https://doi.org/10.1002/(SICI)1099-0763(199706)4:23.3.CO;2-3).
- Bignardi, S., 2017. The uncertainty of estimating the thickness of soft sediments with the HVSR method: a computational point of view on weak lateral variations. *J. Appl. Geophys.* 145C, 28–38. <https://doi.org/10.1016/j.jappgeo.2017.07.017>.
- Bignardi, S., Fiussello, S., Yezzi, A., 2018b. Free and improved computer codes for HVSR processing and inversions. In: 31st Symposium on the Application of Geophysics to Engineering and Environmental Problems, (SAGEEP 2018), Nashville Tennessee, USA March 25–29.
- Bignardi, S., Fedele, F., Santarato, G., Yezzi, A., Rix, G., 2013. Surface waves in laterally heterogeneous media. *J. Eng. Mech.* 139 (9), 1158–1165.
- Bignardi, S., Santarato, G., Abu Zeid, N., 2014. Thickness variations in layered subsurface models — effects on simulated MASW. In: 76th EAGE Conference & Exhibition, <https://doi.org/10.3997/2214-4609.20140540>. Ext. abstract W56-P04.
- Bignardi, S., Mantovani, A., Abu Zeid, N., 2016. OpenHVSR: imaging the subsurface 2D/3D elastic properties through multiple HVSR modeling and inversion. *Comput. Geosci.* 93, 103–113.
- Bignardi, S., Abu Zeid, N., Corradini, E., Santarato, G., 2017. The HVSR technique from array data, speeding up mapping of paleo-surfaces and buried remains: the case of the Bronze-Age site of Pilastris (Italy). In: *SEG Technical Program Exp. Abstracts 2017*, pp. 5119–5124. <https://doi.org/10.1190/segam2017-17746745.1>.
- Bignardi, S., Yezzi, A., Fiussello, S., Comelli, A., 2018a. OpenHVSR — Processing Toolkit: enhanced HVSR processing of distributed microtremor measurements and spatial variation of their informative content. *Comput. Geosci.* 120, 10–20. <https://doi.org/10.1016/j.cageo.2018.07.006>.
- Bignardi, S., Mantovani, A., Rapti, D., Valkaniotis, S., Caputo, R., Yezzi, A., 2019. Mapping and investigating directional effects through analysis of microtremors: the case of palaeo-Piniada valley, central Greece. In: 32nd Symposium on the Application of Geophysics to Engineering and Environmental Problems (SAGEEP 2019), March 17–21, Portland, Oregon USA.
- Bolognesi, M., Furini, A., Russo, V., Pellegrinelli, A., Russo, P., 2014. Accuracy of cultural heritage 3D models by RPAS and terrestrial photogrammetry. *International Archives of the Photogrammetry Remote Sensing and Spatial Information Science* XL 5, 113–119. <https://doi.org/10.5194/isprsarchives-XL-5-113-2014>.
- Bolognesi, M., Furini, A., Russo, V., Pellegrinelli, A., Russo, P., 2015. Testing the low-cost RPAS potential in 3D cultural heritage reconstruction. *International Archives of the Photogrammetry Remote Sensing and Spatial Information Science* XL(5/W4), 229–235. <https://doi.org/10.5194/isprsarchives-XL-5-W4-229-2015>.
- Bonsall, J., Sparrow, T., 2013. NRA archaeological geophysical survey database. <http://www.field2archive.org/nra/>.
- Broglio, A., Tagliacozzo, A., De Stefani, M., Gurioli, F., Facciolo, A., 2006. Aurignacian dwelling structures, hunting strategies and seasonality in the Fumane Cave (Lessinia Mountains). In: *The Early Upper Palaeolithic of Eurasia: General Trends, Local Developments*. State Archaeological Museum-reserve "Kostenki", pp. 263–268.
- Broglio, A., De Stefani, M., Gurioli, F., Pallecchi, P., Giachi, G., Higham, T., Brock, F., 2009. L'art aurignacien dans la décoration de la Grotte de Fumane. *L'Anthropologie* 113, 753–761. <https://doi.org/10.1016/j.anthro.2009.09.016>.
- Cassoli, P.F., Tagliacozzo, A., 1994. Considerazioni paleontologiche, paleoeconomiche e archeozoologiche sui macromammiferi e gli uccelli dei livelli del Pleistocene superiore del Riparo di Fumane (VR) (Scavi 1988-91). *Bollettino Museo Civico di Storia Naturale di Verona* 18, 349–445.
- Clark, A., 2001. *Seeing Beneath the Soil: Prospecting Methods in Archaeology*, 4th edition. Routledge, London.
- Compare et al., 2009. Dietiker B., Pugin, A. J. M. Crow H. L., Skyler Mallozzi, S., Brewer K. D., Cartwright T. J., Hunter J. A., 2018. HVSR measurements in complex sedimentary environment and highly structured resonator topography – comparisons with seismic reflection profiles and geophysical borehole logs. In: 31st Symposium on the Application of Geophysics to Engineering and Environmental Problems, (SAGEEP 2018), Nashville Tennessee, USA March 25–29.
- Cremaschi, M., Ferraro, F., Peresani, M., Tagliacozzo, A., 2005. Il sito: nuovi contributi sulla stratigrafia, la cronologia, le faune a macromammiferi e le industrie del paleolitico antico. In: Broglio, A., Dalmeri, G. (Eds.), *Pitture paleolitiche nelle Prealpi Venete: Grotta di Fumane e Riparo Dalmeri*. Memorie Museo Civico di Storia Naturale

- di Verona, Sezione Scienze dell'Uomo, vol. 9. pp. 12–22.
- Di Giulio, G., Cornou, C., Ohrnberger, M., Wathelet, M., Royelli, A., 2006. Deriving wavefield characteristics and shear-velocity profiles from two-dimensional small-aperture arrays analysis of ambient vibrations in a small Alluvial Basin, Colfiorito, Italy. *Bulletin of Seismological Society of America* 96, 1915–1933. <https://doi.org/10.1785/0120060119>.
- Dietiker, B., Hunter, J.A., 2019. HVSR measurements of two-dimensional subsurface structures — comparisons with seismic reflection profiles. In: 32nd Symposium on the Application of Geophysics to Engineering and Environmental Problems (SAGEEP 2019), March 17–21, Portland, Oregon USA.
- Dietiker, B., Pugin, A.J.M., Crow, H.L., Skyler Mallozzi, S., Brewer, K.D., Cartwright, T.J., Hunter, J.A., 2018. HVSR measurements in complex sedimentary environment and highly structured borehole topography — comparisons with seismic reflection profiles and geophysical borehole logs. In: 31st Symposium on the Application of Geophysics to Engineering and Environmental Problems, (SAGEEP 2018), Nashville Tennessee, USA March 25–29.
- Douka, K., Higham, T.F.G., Wood, R., Boscatto, P., Gambassini, P., Karkanas, P., Peresani, M., Ronchitelli, A., 2014. On the chronology of the Uluzzian. *J. Hum. Evol.* 68, 1–13. <https://doi.org/10.1016/j.jhevol.2013.12.007>.
- Ellwood, B.B., Harrold, F.B., Petruso, K.M., Korkuti, M., 1993. Electrical resistivity surveys as indicators of site potential: examples of a rockhelter in southwestern France and a cave in southern Albania. *Geoarchaeology* 8 (3), 217–227. <https://doi.org/10.1002/gea.3340080304>.
- ERTLab, 2012. 3D electrical resistivity tomography inversion software, user manual. www.geostudiastier.it. www.mpt3d.com.
- Fiore, I., Gala, M., Romandini, M., Cocca, E., Tagliacozzo, A., Peresani, M., 2016. From feathers to food: reconstructing the complete exploitation of avifaunal resources by Neanderthals at Grotta di Fumane, unit A9. *Quat. Int.* 421, 134–153.
- Guéguen, P., Cornou, C., Garambois, S., Banton, J., 2007. On the limitation of the HVSR spectral ratio using seismic noise as an exploration tool: application to the Grenoble Valley (France), a small apex ratio basin. *Pure Appl. Geophys.* 164, 115–134. <https://doi.org/10.1007/s00024-006-0151-x>.
- Higham, T.F.G., Brock, F., Peresani, M., Broglio, A., Wood, R., Douka, K., 2009. Problems with radiocarbon dating the Middle and Upper Palaeolithic transition in Italy. *Quat. Sci. Rev.* 28, 1257–1267. <https://doi.org/10.1016/j.quascirev.2008.12.018>.
- Jol, H.M., Schroder, J.F., Reeder, P., Freund, R.A., 2002. Return to the cave of letters (Israel): a ground penetrating radar archaeological expedition. In: Noon, D.A., Stickley, G.F., Longstaff, D. (Eds.), *Proceedings of the Eighth International Conference on Ground Penetrating Radar (GPR 2000)*. SPIE 4084, pp. 882–886.
- Konno, K., Ohmachi, T., 1998. Ground-motion characteristics estimated from spectral ratio between horizontal and vertical components of microtremor. *Bull. Seism. Soc. Am.* 88-1, 228–241.
- Lancioni, G., Bernetti, R., Quagliarini, E., Tonti, L., 2014. Effects of underground cavities on the frequency spectrum of seismic shear waves. *Advances in Civil Engineering* 2014, 1–17. <https://doi.org/10.1155/2014/934284>.
- López-García, J.M., Dalla Valle, C., Cremaschi, M., Peresani, M., 2015. Reconstruction of the Neanderthal and Modern Human landscape and climate from the Fumane cave sequence (Verona, Italy) using small-mammal assemblages. *Quat. Sci. Rev.* 128, 1–13. <https://doi.org/10.1016/j.quascirev.2015.09.013>.
- Mantovani, A., Abu Zeid, N., Bignardi, S., Tarabusi, G., Santarato, G., Caputo, R., 2019. Seismic noise-based strategies for emphasizing the recent tectonic activity of blind thrusts: the case of the Ferrara Arc, Northern Italy. *Pure Appl. Geophys.* <https://doi.org/10.1007/s00024-019-02120-8>.
- Martini, M., Sibilia, M., Croci, S., Cremaschi, M., 2001. Thermoluminescence (TL) dating of burnt flints: problems, perspectives and some example of application. *J. Cult. Herit.* 2, 179–190. [https://doi.org/10.1016/S1296-2074\(01\)01126-8](https://doi.org/10.1016/S1296-2074(01)01126-8).
- Matsushima, S., Hirokawa, T., De Martin, F., Kawase, H., Sánchez-Sesma, F.J., 2014a. The effect of lateral heterogeneity on horizontal-to-vertical spectral ratio of microtremors inferred from observation and synthetics. *Bull. Seismol. Soc. Am.* 104 (1), 381–393. <https://doi.org/10.1785/0120120321>.
- Matsushima, S., Hirokawa, T., De Martin, F., Kawase, H., Sánchez-Sesma, F.J., 2014b. The effect of lateral heterogeneity on horizontal-to-vertical spectral ratio of microtremors inferred from observation and synthetics. *Bull. Seismol. Soc. Am.* 104 (1), 381–393. <https://doi.org/10.1785/0120120321>.
- Morelli, G., LaBrecque, D.J., 1996. Advances in ERT inverse modelling. *European Journal of Environmental and Engineering Geophysical Society* 1, 171–186.
- Nakamura, Y., 1988. A method for dynamic characteristics estimation of subsurface layers using microtremor on the surface. In: *RTRI Report 2*. vol. 4. pp. 18–27 (in Japanese with English abstract).
- Nakamura, Y., 1989. A method for dynamic characteristics estimation of subsurface using microtremor on the ground surface. *Quarterly Report of RTRI* 30 (1), 25–33.
- Nakamura, Y., 2000. Clear identification of fundamental idea of Nakamura's technique and its applications. In: *The 12th World Conference on Earthquake Engineering*, (2656, Auckland, New Zealand, 30 January–4 February, 2000).
- Nakamura, Y., 2008. On the HVSR Spectrum. In: *The 14th World Conference on Earthquake Engineering*, October 12–17, Beijing, China.
- Nakamura, Y., 2019. What is the Nakamura method? *Seismol. Res. Lett.* 90 (4), 1437–1443. <https://doi.org/10.1785/0220180376>.
- Nakamura, Y., Ueno, M., 1986. A simple estimation method of dynamic characteristics of subsoil. In: *Proceedings of the 7th Japan Earthquake Engineering Symposium 1986*, Dec., 1986, pp. 265–270 (in Japanese with English abstract).
- Nehmé, C., Voisin, C., Mariscal, A., Gérard, P.C., Cornou, C., Jabbour-Gédéon, B., Amhaz, S., Salloum, N.B.S., Adjizian, A.G., Delannoy, J.J., 2013. The use of passive seismological imaging in speleogenetic studies: an example from Kanaan Cave, Lebanon. *Int. J. Speleol.* 42 (2), 97–108.
- Obradović, M., Abu Zeid, N., Bignardi, S., Bolognesi, M., Peresani, M., Russo, P., Santarato, G., 2015. High resolution geophysical and topographical surveys for the characterisation of Fumane Cave prehistoric site, Italy. In: *Near Surface Geoscience 2015 — 21st European Meeting of Environmental and Engineering Geophysics*, Tourin, Italy. vol. Volume: Mo 21 B07.
- Oldenburg, D.W., Li, Y., 1999. Estimating depth of investigation in dc resistivity and IP surveys. *Geophysics* 64 (2), 403–416.
- Orlando, L., 2013. GPR to constrain ERT data inversion in cavity searching: theoretical and practical applications in archaeology. *J. Appl. Geophys.* 89, 35–47. <https://doi.org/10.1016/j.jappgeo.2012.11.006>.
- Ortega, A.I., Benito-Calvo, A., Porres, J., Pérez-González, A., Martín Merino, M.A., 2010. Applying electrical resistivity tomography to the identification of endokarstic geometries in the Pleistocene sites of the Sierra de Atapuerca (Burgos, Spain). *Archaeol. Prospect.* 17, 233–245. <https://doi.org/10.1002/arp.392>.
- Papadopoulos, N.G., Tsourlos, P., Tsokas, G.N., Sarris, A., 2006. Two-dimensional and three-dimensional electrical imaging in archaeological site investigation. *Archaeol. Prospect.* 13, 163–181. <https://doi.org/10.1002/arp.276>.
- Papadopoulos, N.G., Yi, M.J., Kim, J.H., Tsourlos, P., Tsokas, G.N., 2010. Geophysical investigation of tumuli by means of surface 3D electrical resistivity tomography. *J. Appl. Geophys.* 70, 192–205. <https://doi.org/10.1016/j.jappgeo.2009.12.001>.
- Peresani, M., 2012. Fifty thousand years of flint knapping and tool shaping across the Mousterian and Uluzzian sequence of Fumane cave. *Quat. Int.* 247, 125–150. <https://doi.org/10.1016/j.quaint.2011.02.006>.
- Peresani, M., Cremaschi, M., Ferraro, F., Falguères, C., Bahain, J.J., Gruppioni, G., Sibilia, E., Quarta, G., Calcagnile, L., Dolo, J.M., 2008. Age of the final Middle Palaeolithic and Uluzzian levels at Fumane Cave, Northern Italy, using ¹⁴C, ESR, ²³⁴U/²³⁰Th and thermoluminescence methods. *J. Archaeol. Sci.* 35 (11), 2986–2996. <https://doi.org/10.1016/j.jas.2008.06.013>.
- Peresani, M., Chrzavetz, J., Danti, A., de March M., Duches R., Gurioli F., Muratori S., Romandini M., Trombino L., Tagliacozzo A., 2011. Fire places, frequentations and the environmental setting of the final Mousterian at Grotta di Fumane: a report from the 2006–2008. *Quartär* 58: 131–151.
- Peresani, M., Cristiani, E., Romandini, M., 2016. The Uluzzian technology of Grotta di Fumane and its implication for reconstructing cultural dynamics in the Middle–Upper Palaeolithic transition of Western Eurasia. *J. Hum. Evol.* 91, 36–56. <https://doi.org/10.1016/j.jhevol.2011.03.028>.
- Peresani, M., Delpiano, D., Duches, R., Gennai, J., Marazzan, D., Nannini, N., Romandini, M., Aleo, A., Cocilova, A., 2017. Il Musteriano delle unità A10 e A11 a Grotta di Fumane (VR). Risultati delle campagne di scavo 2014 e 2016. In: *Fasti Online Documents & Research*. vol. 397. pp. 1–13.
- Piro, S., Mauriello, P., Cammarano, F., 2000. Quantitative integration of the geophysical methods for archaeological prospection. *Archaeol. Prospect.* 7 (4), 203–213. [https://doi.org/10.1002/1099-0763\(200012\)7:4<203::AID-ARP133>3.0.CO;2-T](https://doi.org/10.1002/1099-0763(200012)7:4<203::AID-ARP133>3.0.CO;2-T).
- Quarto, R., Schiavone, D., Diaferia, I., 2007. Ground penetrating radar survey of a prehistoric site in southern Italy. *J. Archaeol. Sci.* 34, 2071–2080.
- Romandini, M., Nannini, N., Tagliacozzo, A., Peresani, M., 2014. The ungulate assemblage from layer A9 at Grotta di Fumane, Italy: a zooarchaeological contribution to the reconstruction of Neanderthal ecology. *Quat. Int.* 337, 11–27. <https://doi.org/10.1016/j.quaint.2014.03.027>.
- Roy, A., Apparao, A., 1971. Depth of investigation in direct current methods. *Geophysics* 36, 943–959 (studies: an example from Kanaan Cave, Lebanon).
- Schmidt, A., Ermenwein, E., 2011. *Guide to Good Practice: Geophysical Data in Archaeology*, 2nd edition. Archaeology Data Service.
- SESAME European Project, 2004. *Site Effects Assessment Using Ambient Excitations; Deliverable D23.12: Guidelines for the Implementation of the H/V Spectral Ratio Technique on Ambient Vibrations: Measurements, Processing and Interpretation; Deliverable D13.08. Final report WP08. Nature of Noise Wavefield*.
- Shopov, Y., Stoykova, D., Petrova, A., Vasiliev, V., Tsankov, L., 2008. Potential and limitations of the archaeo-geophysical techniques. In: Kostov, R.I., Gaydarska, B., Gurova, M. (Eds.), *Proceedings of the International Conference, 29–30 October 2008, Geoarchaeology and Archaeomineralogy*. Sofia, Publishing House “St. Ivan Rilski”, Sofia, pp. 320–324.
- Tikhonov, A.N., Arsenin, V.Y., 1977. *Solutions of Ill-posed Problems*. Winston and Sons, Washington (DC).
- Tsokas, G.N., Tsourlos, P.I., Papadopoulos, N., 2009. Electrical resistivity tomography: a flexible technique in solving problems of archaeological research. In: Campana, S., Piro, S. (Eds.), *Seeing the Unseen. Geophysics and Landscape Archaeology*. Taylor & Francis, London.